Biosensors and Bioelectronics 85 (2016) 422–428

Contents lists available at ScienceDirect

Biosensors and Bioelectronics

journal homepage: www.elsevier.com/locate/bios

# An immunochromatographic biosensor combined with a water-swellable polymer for automatic signal generation or amplification

Kahee Kim [a,1], Hyou-Arm Joung [a,1,2], Gyeo-Re Han [a], Min-Gon Kim [a,b,*]

[a] Department of Chemistry, Gwangju Institute of Science and Technology (GIST), 123 Cheomdangwagi-ro, Buk-gu, Gwangju 61005, Republic of Korea
[b] INGIbio Co. Ltd., R&D Center, 206, APRI, 123 Chemdangwagi-ro, Buk-gu, Gwangju 61005, Republic of Korea

ARTICLE INFO

*Article history:*
Received 23 December 2015
Received in revised form
18 April 2016
Accepted 29 April 2016
Available online 4 May 2016

*Keywords:*
Automatic sequential reaction
Lateral flow immunoassay
Signal amplification
Water-swellable polymer
Chemiluminescence
C-reactive protein

ABSTRACT

An immunochromatographic assay (ICA) strip is one of the most widely used platforms in the field of point-of-care biosensors for the detection of various analytes in a simple, fast, and inexpensive manner. Currently, several approaches for sequential reactions in ICA platforms have improved their usability, sensitivity, and versatility. In this study, a new, simple, and low-cost approach using automatic sequential-reaction ICA strip is described. The automatic switching of a reagent pad from separation to attachment to the test membrane was achieved using a water-swellable polymer. The reagent pad was dried with an enzyme substrate for signal generation or with signal-enhancing materials. The strip design and system operation were confirmed by the characterization of the raw materials and flow analysis. We demonstrated the operation of the proposed sensor by using various chemical reaction-based assays, including metal-ion amplification, enzyme-colorimetric reaction, and enzyme-catalyzed chemiluminescence. Furthermore, by employing C-reactive protein as a model, we successfully demonstrated that the new water-swellable polymer-based ICA sensor can be utilized to detect biologically relevant analytes in human serum.



## 1. Introduction

Point-of-care (POC) diagnostic sensors have many advantages, including cost-effectiveness, simplicity, and rapid operation. Additionally, POC diagnostic testing increases the efficiency of the clinical process relative to central laboratory testing (Von Lode, 2005). Compared with central laboratory methods, POC diagnostic sensors have limitations in diagnostic accuracy owing to several drawbacks, including environmental effects, sample-handling errors, poor analytical performance, and post-test analysis (documentation) (Kost et al., 1999; Von Lode, 2005). In this regard, studies in the field of POC diagnostic sensors aim to overcome these drawbacks and have led to the design of microfluidic devices (Ko et al., 2008; Krejcova et al., 2014; Obubuafo et al., 2008) miniaturized total-analysis systems (Abrams et al., 2007; Chin et al., 2011; Qiu et al., 2009) and microfluidic paper-based analytical devices (He and Liu, 2013; Liu and Crooks, 2011; Martinez et al., 2007) as future alternatives (Tüdős et al., 2001). However, these technologies are not candidates for immediate commercialization owing to their relatively high costs, complex processing, and lack of verification (Su et al., 2015).

Among the commercialized POC diagnostic sensors, immunochromatographic assay (ICA) strip sensors are well-established immunoassay sensor platforms that are widely used beyond the clinical diagnostic field (Yetisen et al., 2013). Various types of ICAs have been used as diagnostic sensors for the detection of proteins (Cho and Paek, 2001; Oh et al., 2014), bacteria (Fang et al., 2014; Yu et al., 2011), viruses (Al-Yousif et al., 2002; Zhang et al., 2015), nucleic acids (Hu et al., 2013; Liu et al., 2013), and toxic molecules (Song et al., 2014; Wang et al., 2006). However, conventional ICA sensors using gold nanoparticles have drawbacks in the level of detection sensitivity and the quantitative assays that are required for precise diagnostic applications (Myers and Lee, 2008; Posthuma-Trumpie et al., 2009). To overcome these problems, various studies have refined signal-amplification or sensitive signal-generation methods, such as metal-ion signal amplification (Anfossi et al., 2013; Li et al., 2013), chemiluminescence assays (Kim et al., 2010; Mirasoli et al., 2012), and enzyme-colorimetric reactions (Kawde et al., 2010; Parolo et al., 2013; Samsonova et al., 2015) using ICA strip sensors. Additionally, several approaches attempted automatic reactions in a sensor using simple fluid technology or paper networks. For example, a plastic enzyme-linked immunosorbent

* Corresponding author at: Department of Chemistry, Gwangju Institute of Science and Technology (GIST), 123 Cheomdangwagi-ro, Buk-gu, Gwangju 61005, Republic of Korea.
*E-mail address:* mkim@gist.ac.kr (M.-G. Kim).
[1] These authors contributed equally to this work.
[2] Present address: Department of Electrical Engineering, University of California, Los Angeles, CA 90095, USA.

http://dx.doi.org/10.1016/j.bios.2016.04.096
0956-5663/

assay (ELISA)-on-a-chip method employed a cross-flow of solution containing an enzyme substrate to detect cardiac troponin I (Cho et al., 2006). A two-dimensional paper-network (2DPN) format was also developed to enable multistep assays to be performed simply (Fu et al., 2012). Toley et al. (2015) reported a paper-microfluidic device that automatically controlled fluids using expandable elements. This device used water to expand the compressed sponges, which enabled the sponges to connect or disconnect by two pathways. Even though these methods increased the detection sensitivity of the ICA strip sensor, additional operational steps, such as multistep injection and/or washing, offset the advantages of the ICA sensor. We previously reported an automatic enzyme immunoassay based on ICA methods that utilized an asymmetric polysulfone membrane (ASPM) (Joung et al., 2014). In this sensor, the horizontal flow at the small-pore side was stronger than that at the large-pore side. Consequently, the ASPM delayed the release of the secondary reagents following the immune reaction. Moreover, this platform was adapted to an ICA strip format that did not require additional fluidic support. However, this sensor was limited by its use of the conjugation pad owing to the difficulty in separating conjugates and secondary reagents during sensor operation.

Here, we demonstrated a fully automated immunochromatographic sensor performing ELISA or second-signal enhancing immunoassays without an additional supporting apparatus. A key design element involved automatically switching the reagent pad from separation to attachment to the test membrane. The reagent pad was dried with an enzyme substrate for signal generation or with signal-enhancing materials. The automatic switching was accomplished by using a water-swellable polymer composed of polyvinyl alcohol. As shown in Fig. 1, the aqueous sample that was dropped onto the sample pad soaked and gradually swelled the water-swellable polymer. After a few minutes, the reagent pad below the water-swellable polymer came into contact with the test membrane, which was followed by the release of the secondary reagent from the reagent pad to the test membrane to generate or amplify the immunoassay signal. The feasibility of this strategy was demonstrated by the results obtained following the screening of various water-soluble tapes and the new ICA sensor in combination with a water-swellable polymer tape applied to various chemical reaction-based assays, such as metal-ion amplification, enzyme-colorimetric reactions, and enzyme-catalyzed chemiluminescence. Finally, the practical application of the developed biosensor coupled with a chemiluminescence assay was demonstrated by the detection of C-reactive protein (CRP) in human serum.

## 2. Materials and methods

### 2.1. Materials

CRP-free serum (90R-100) and surfactant 10G (95R-103) were purchased from Fitzgerald Industries International (Acton, MA,

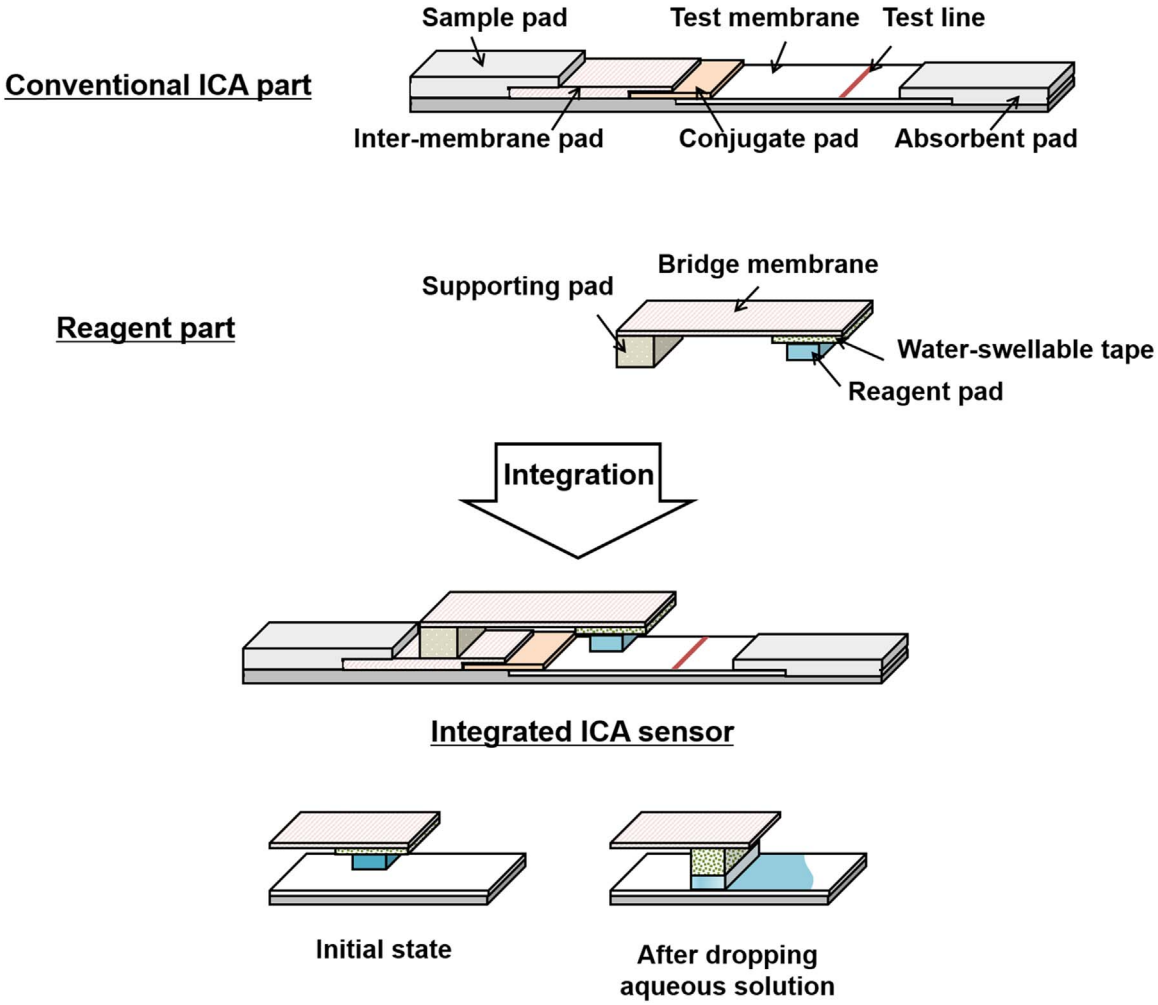


**Fig. 1.** Schematic illustrations of the suggested structure for the automatic sequential reactions. The water-swellable polymer was swelled and then switched the flow to the secondary reagent by aqueous solution.

USA). CRP (236608), and nitrocellulose (NC) (HFB12004) membranes were purchased from Merck Millipore (Darmstadt, Germany). Anti-CRP polyclonal antibody (ab31156), monoclonal antibody horseradish peroxidase (HRP) conjugate (ab24461), and anti-choline oxidase antibody (ab34489) were purchased from Abcam Inc. (Cambridge, MA, USA). Two types of cellulose absorbent pad (Absorbent type 133 and 165 with the thickness, 825.5 and 1836.1 μm, respectively.) and asymmetric polysulfone membrane (vivid plasma separation-GX) were obtained from Pall Co. (Port Washington, NY, USA). Single layer matrix membrane (Fusion 5) was purchased from GE Healthcare Life Sciences (Little Chalfont, Buckinghamshire, UK). Water-swellable tape (57-899) was purchased from Clover Manufacturing Co., Ltd. (Osaka, Japan), and water-soluble tape (hydrolysis adhesive tape) was from Deobureo Industries (Gyeonggi-do, South Korea). Human troponin I antibody-HRP conjugate was purchased from HyTest Ltd. (Turku, Finland). Gold colloid solution was purchased from BB International (EM.GC 15, EM. GC 40; Cardiff, UK). The alkaline phosphatase (AP)-conjugate substrate kit used in the enzyme-colorimetric assay was purchased from Bio-Rad (Hercules, CA, USA), and AP-conjugated streptavidin (21324) was purchased from Thermo Scientific (Rockford, MD, USA). Choline oxidase was purchased from Toyobo Company Ltd. (Osaka, Japan). Luminol, choline chloride, p-coumaric acid, polyvinylpyrrolidone (PVP; 10 K and 55 K), gold (III) chloride trihydrate, hydroxylamine hydrochloride, and other chemicals were purchased from Sigma-Aldrich (St. Louis, MO, USA).

### 2.2. Instruments

The drying oven (KO-100) was obtained from Korea Auto Control & Scientific Instrument Co. (Seoul, South Korea). A cutter device (TBC-50TS; cuTex, Gyeonggi-do, South Korea) was used for cutting membranes. A dispenser (DCI100; Zeta Corporation, Gyeonggi-do, South Korea) was used to immobilize antibodies on the test and control lines, and a HANIL microcentrifuge (micro17TR; Quasar Instruments, Colorado Springs, CO, USA) was used to separate gold nanoparticles (AuNPs). A microscope (Olympus BX43, Tokyo, Japan) was used to observe the surface structure of the water-swellable tapes. All buffers and reagent solutions were prepared with water purified using PURELAB Option-Q (ELGA LabWater). All signals, such as color and luminescence, were measured using the ChemiDoc MP image system (Bio-Rad) and analyzed using Image Lab 4.0 software (Bio-Rad).

### 2.3. Characterization of water-swellable tape

Water-swellable tape ($4.0 \times 8.0\ mm^2$) was attached to the NC membrane as a conventional strip. Phosphate-buffered saline (PBS; 100 μL) was loaded onto the sample pad, and then changes in the height of the tape were measured over a 20 min period. After 10 min, the height and length were measured and compared with those before solution injection.

The porous structures of the water-soluble tapes were visualized using microscopy. Each water-soluble tape was attached to the slide glass and observed before water treatment and after 50 μL distilled water was dropped onto the water-soluble tape and it was covered with a cover glass. The porous structure was observed using microscopy during the 10 min interval.

### 2.4. Preparation of the new ICA sensor combined with water-swellable polymer

The new sensor was comprised of two major components: a conventional ICA structure and an additional structure for carrying out sequential reactions. The conventional ICA structure was composed of a sample pad, inter-membrane pad, conjugate pad, test membrane, and absorbent pad. The platform for carrying out the sequential reactions was comprised of a supporting pad, bridge membrane, water-swellable tape, and reagent pad. The sample pad, absorbent pad, and reagent pad were made of absorbent type 133, and Fusion 5 was used for the conjugate pad. NC membrane was used for the test membrane, and absorbent type 165 was used for the supporting pad. A vivid plasma separation-GX membrane was used as the inter-membrane pad and bridge membrane.

The overall structure of the new ICA sensor combined with the water-swellable polymer is depicted in Fig. 1. An absorbent pad ($4.0 \times 20\ mm^2$) was attached to the top of the NC membrane ($4.0 \times 25\ mm^2$) and then the conjugate pad ($4.0 \times 8.0\ mm^2$), inter-membrane pad ($4.0 \times 15\ mm^2$), and sample pad ($4.0 \times 25\ mm^2$) were consecutively assembled on a plastic-adhesive backing, with the smaller pore side of the inter-membrane pad oriented toward the upper side. The bridge membrane ($4.0 \times 20\ mm^2$) was attached to the slide glass using double-sided tape, and then the water-swellable tape was attached to the bridge membrane to enable the larger pore side of the bridge membrane to make contact with the water-swellable tape. The reagent pad was attached to the water-swellable tape with the side of the treated sealing tape that was making contact with the water-swellable tape. The assembled strip was immobilized on a plate with both sides of the strip serving as barriers for assembling the slide glass. The glass slide was then placed on the barriers and the supporting pad ($4.0 \times 3.0\ mm^2$) and then immobilized using double-sided tape.

### 2.5. Flow analysis of the new ICA sensor combined with water-swellable polymer

Analysis of the flow through the new ICA sensor was carried out by monitoring the release of two dyes in the reagent pad attached to the water-swellable tape and the conjugate pad. Blue and red dye solutions containing 1% (v/v) S10G were used to visualize flow. The flow of the red dye represented an immunoassay on the test membrane, while the blue dye (1% (v/v) S10G) flowing through the system was monitored as a function of time.

### 2.6. Operation of various second reactions

#### 2.6.1. Reagent pad preparation

Various reagents were tested as components for different signal-producing reactions. These included color dye, luminol, gold ions, and nitro blue tetrazolium/5-bromo-4-chloro-3-indolyl-phosphate (NBT/BCIP) for bringing about respective signals, including flow analysis, chemiluminescence, metal-ion amplification, and enzyme-colorimetric reactions. All secondary reagents [color dye including 1% surfactant 10 G (S10G), 50 mM luminol, 0.1 M gold ions, and NBT/BCIP in a mixture of the AP kit in a 5:2 ratio] were prepared in the following manner: each secondary reagent solution (65 μL) was dropped on the sample pad ($4.0 \times 20\ mm^2$), which was then dried at 65 °C for 30 min, and the pad was attached to a sealing tape, which was cut to obtain a $4.0 \times 3.8\ mm^2$ section. This method is described in detail below.

#### 2.6.2. Gold-ion signal amplification

To carry out a metal-ion amplification assay, the gold-ion amplification method was used in the new ICA sensor combined with the water-swellable polymer. A solution of gold(III) chloride trihydrate [0.1 M in 0.1 M phosphate buffer (pH 7.4)] was applied to the reagent pad, which was then dried. The loading solution contained 10 mM hydroxylamine hydrochloride in 0.1 M Tris–HCl (pH 8.0) as the reducing agent. Various concentrations of AuNPs (15 nm) were spotted (1 μL) onto the test membrane.

*2.6.3. Enzyme-colorimetric reaction*

Reaction of NBT and BCIP promoted by AP was selected as the colorimetric process. A solution containing 50 μL NBT and 20 μL BCIP was mixed with 930 μL 0.5 M Tris–HCl buffer (pH 9.5) and applied to the reagent pad, which was then dried. Tris–HCl buffer (0.1 M, pH 8.5) was used as the injection solution. Various concentrations of streptavidin-labeled AP (1 μL) were spotted on the NC membrane.

*2.6.4. Chemiluminescence reaction*

Chemiluminescence was implemented with reactions between choline and choline oxidase for generation of hydrogen peroxide ($H_2O_2$). A solution containing 10 μL anti-choline oxidase antibody (10 mg/mL) and 2.5 μL choline oxidase (10 mg/mL) was mixed with 37.5 μL 0.1 M Tris–HCl (pH 8.5), and then spotted (1 μL) onto the test membrane between the capture antibody and reagent pad. The components of the chemiluminescent substrates were those developed in our earlier work (Joung et al., 2014). Briefly, a solution containing 100 μL luminol (0.5 M in 50 mM NaOH), 30 μL choline chloride (1 M in distilled water), and 1 μL p-coumaric acid (0.5 M in dimethylformamide) was mixed with 870 μL 0.1 M Tris–HCl buffer (pH 8.5). After mixing, 65 μL of the solution was applied to the sample pad, which was then dried. Solutions (1 μL) of various concentrations of HRP-labeled antibodies and choline oxidase antibody were spotted onto the test membrane. The loading solutions contained 0.5% (v/v) S10G and 1% (w/v) PVP 10 K in 0.1 M Tris–HCl (pH 8.5). The resulting solution was loaded onto the sample pad and changes in signal intensities were measured over a 20 min period.

*2.7. Detection of CRP in human serum*

The CRP-capture antibody (1 μL/cm) was immobilized, dried at 37 °C for 15 min, and 0.05% (v/v) S10G was applied to the 120 s/cm NC membrane. Solutions containing various CRP concentrations were prepared in CRP-free human-serum solution. The solutions (180 μL) were applied to the strip sensor and the signal intensities were measured over a 20-min period.

Additionally, results obtained with the new assay method were compared with those obtained with a conventional ICA. The procedure described by Oh et al. (2014) was employed to prepare the required AuNP-conjugate. Anti-CRP antibody diluted in PBS (10 μL, 1 mg/mL) was added to a mixture of 900 μL 40 nm AuNP and 100 μL 0.1 M borate buffer (pH 8.5). After incubation for 30 min at room temperature, 100 μL of 100 mg/mL bovine serum albumin (BSA) in PBS was added to the mixture to block the AuNP surface. After incubation for 60 min at room temperature, the mixture was centrifuged at 8000 rpm at 10 °C for 20 min. The supernatant was discarded and the AuNP conjugate was resuspended in 10 mM borate buffer containing 1 mg/mL BSA (pH 8.5). The centrifugation and resuspension steps were repeated twice using 10 mM borate buffer. The resulting AuNP conjugate was suspended in 10 mM borate buffer (pH 8.5), diluted two-fold with the solution containing 2% (w/v) PVP 10 K and 1% (v/v) S10G in PBS, and applied (5 μL) to the conjugate pad, which was dried at 37 °C for 15 min. A strip was assembled, and the sample pad was loaded with 100 μL. The signal intensity was measured after 15 min.

## 3. Results and discussion

*3.1. System operation principle and characterization*

The immunochromatographic biosensor combined with a water-swellable polymer is schematically described in Fig. 1. The sensor system is composed of two parts—the conventional ICA part and the reagent part. The reagent part includes the reagent pad, the water-swellable tape, the bridge membrane, and the supporting pad. When an aqueous sample solution is loaded onto the sample pad, the target antigens bind to the detection antibodies to form a complex in the conjugate pad. The passage of the complex through the NC membrane enables the complex to bind to the capture antibodies in the test line. At the same time, the solution is absorbed onto the supporting pad and transferred to the water-swellable tape. Finally, after a certain period along the test membrane, the secondary reagents in the reagent pad are released because of the expansion of the water-swellable tape, which creates contact between the reagent pad and the test membrane. A detailed illustration about the flow direction of the proposed ICA sensor is described in Fig. S1.

The water-swellable tape was used as a key component in the reagent part. In order to confirm the expanding effect of the water-swellable tape, the tape was attached to the middle of the NC membrane and a PBS buffer was loaded onto the sample pad located on one end of the NC membrane. As a result, we observed that the contact area of the tape gradually shrunk as the height increased (Fig. 2A), and the final height was measured as $1.1 \pm 0.1$ mm (Fig. 2B). Many air pockets were observed in the water-swellable tape used in this study (Fig. S2A); the air pockets gradually shrunk or disappeared following contact with the aqueous solution. The presence of the air pockets was the driving force causing shrinkage of the water-swellable tape. When no air pockets were observed in the water-soluble tape, expanding effect did not occur (Fig. S2B). Additionally, the contact timing of the reagent pad controlled the pore size and thickness of the bridge membrane. As shown in Fig. 2C, the time required for a 0.6-mm

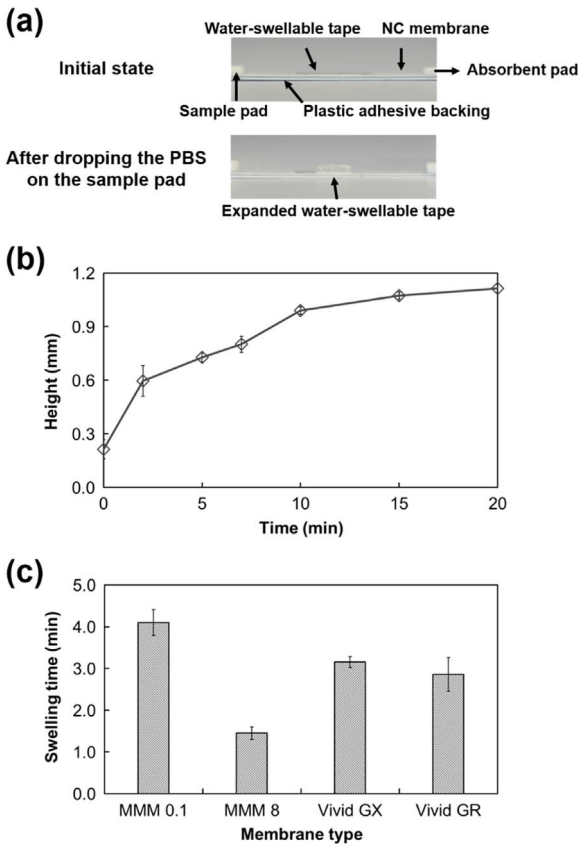


**Fig. 2.** Characterization of the water-swellable tape. (a) Photograph of the water-swellable tape before and after water treatment. (b) The height change of the water-swellable tape depending on time after water treatment. (c) The time required for the water-swellable tape to swell to 0.6 mm, depending on the membrane type.

increase in height was confirmed to be dependent upon the type of bridge membrane, specifically upon the pore size and thickness (Table S1). Overall, it was found that the water-swellable tape contained lateral-shrinking properties owing to its porous structure, and it underwent a vertical expansion in water. Therefore, the expansion of the water-swellable tape brought the reagents and reactant of the sequential reaction into contact in an automatic manner without further inputs. Additionally, we confirmed that lot-to-lot variation and environmental humidity effect during the operation of the water-swellable tapes were negligible (Fig. S3 and Fig. S4).

### 3.2. Operation of the developed ICA sensor in various reagents

ICAs are generally used to detect specific target analytes by employing a one-step sample injection. This is one of the most important advantages of ICAs. However, this advantage is a limiting factor in applying this method to various high-sensitivity assays, such as metal-ion amplification, enzyme-colorimetric reactions, and enzyme-catalyzed chemiluminescence. If it were possible to enable the ICA strip to operate in one-step in a simple and low-cost manner, the opportunities to utilize these assays in various diagnostic sensors would be significantly increased.

The sequential flows in the new ICA sensors combined with the water-swellable polymers are divided into four steps: 1) sample injection, 2) reaction-membrane flow and tape swelling, 3) touching the reagent pad and releasing reagents, and 4) reagent flow. In order to confirm these four sequential flows, the blue dye-treated reagent pad was used. As shown in Fig. 3A, these four steps were observed after sample injection (supplementary movie S1). Additionally, gold-ion amplification, the NBT/BCIP-colorimetric reaction, and enzyme-catalyzed chemiluminescence were investigated to assess the versatility of the ICA sensor combined with the water-swellable polymer. Gold-ion amplification involves

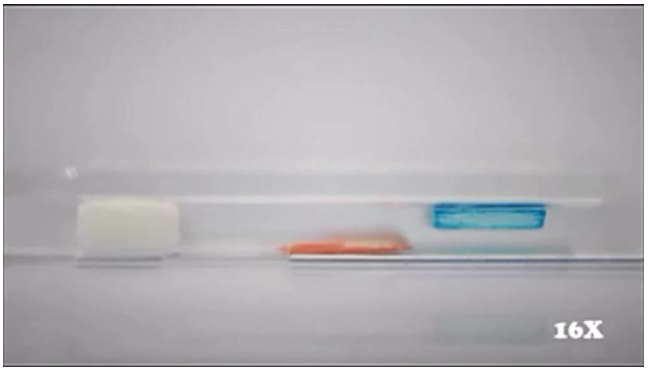


**Movie S1.** Operation of the ICA sensor combined with a water-swellable polymer. A video clip is available online.Supplementary material related to this article can be found online at http://dx.doi.org/10.1016/j.bios.2016.04.096.

the surface-catalyzed reduction of $Au^{3+}$ by hydroxylamine ($NH_2OH$). Upon reduction of the $Au^{3+}$ ion by $NH_2OH$, AuNPs are formed and the size of the AuNPs increases (Brown and Natan, 1998; Soni and Mehrotra, 2003). Many ICA signal-amplification methods based on this process have been reported (Fu et al., 2012; Li et al., 2013; Toley et al., 2015). To apply this method to the new ICA sensor combined with the water-swellable polymer, $NH_2OH$ was present in the solution and $Au^{3+}$ was deposited on the reagent pad. The $NH_2OH$ solution flowed past the test membrane at the same time that the water-swellable tape gradually expanded. After a few minutes, the gold ions on the reagent pad came into contact with the test membrane and the gold ions were released. The reaction with the AuNPs on the test membrane led to an amplified AuNP signal. Because the water-swellable tape delayed the contact time between the gold ions and $NH_2OH$, the amplified signal appeared in the absence of other undesirable signals. As shown in Fig. 3B, the amplified signal intensities were linearly

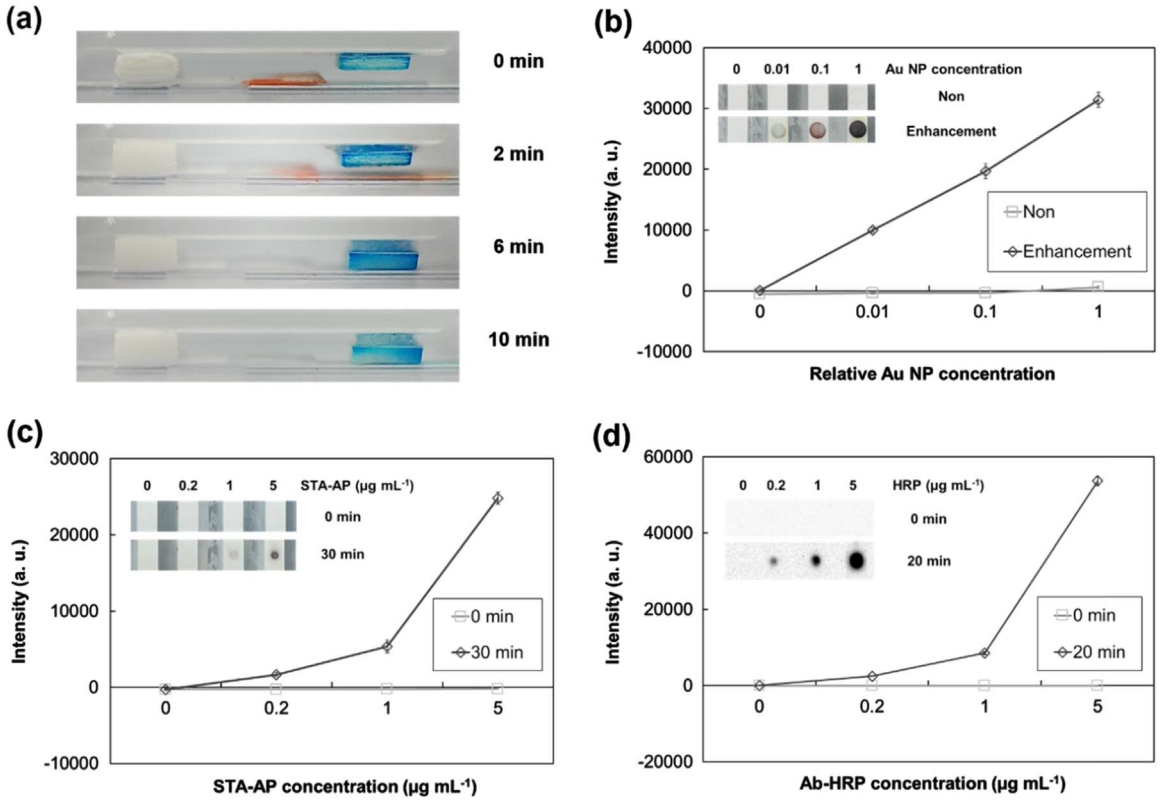


**Fig. 3.** Implementation of automatic sequential reactions. (a) Flow analysis using color dye, (b) gold ion amplification, (c) NBT/BCIP colorimetric reaction and (d) enzymatic catalyzed chemiluminescence in the new ICA sensor combined water-swellable polymer.

dependent upon the AuNP concentration. The reaction of NBT and BCIP catalyzed by AP was selected as the enzyme-colorimetric reaction. This reaction is primarily used in immunoblotting, *in situ* hybridization, and immunohistochemistry (Blake et al., 1984) and produces an insoluble NBT diformazan end product associated with a color change from blue to purple that can be observed by the naked eye. The enzyme-catalyzed reaction between NBT and BCIP requires a high pH, a condition that is unsuitable for most immunoassays. In the new ICA sensor combined with a water-swellable polymer, a high-pH solution of NBT/BCIP was applied to the reagent pad and the pad was then dried. Initially, the sample solution flowed through the membrane and the NBT/BCIP mixture was released by the expansion of the water-swellable tape. The pH of the test membrane was altered upon contact with the reagent pad, thus enabling the NBT/BCIP reaction. Similar to the result observed with the gold-ion amplification, the signal intensity of the streptavidin-labeled AP increased when the AP concentration increased (Fig. 3C). For the enzyme-catalyzed chemiluminescence signaling, we utilized the reaction of choline promoted by choline oxidase to generate $H_2O_2$ (Joung et al., 2014; Leca et al., 2001). In this process, luminol reacts with $H_2O_2$ in the presence of HRP to generate light. Using the ICA sensor combined with the water-swellable polymer, choline was present on the reagent pad containing the other chemicals, and choline oxidase was immobilized on the test membrane between the conjugate pad and the reagent pad. The choline released from the reagent pad reacted with the choline oxidase to form $H_2O_2$, which then reacted with the HRP bound to the test line. This sequence produced a chemiluminescent signal. Time dependent chemiluminescence signal change was shown in Fig. S5. The signal intensities varied slightly in the early time phase despite using the same concentration of the antibody-HRP, but after 20 min the signal reached a level value with no more than a 5% coefficient of variation (CV) and maintained a similar level up to the end of measurement. So, the detection time was selected at 20 min. The chemiluminescent signal intensity measured at 20 min increased with the concentration of HRP (Fig. 3D).

Studies were conducted to evaluate the use of the new ICA sensor combined with the water-swellable polymer in a variety of chemical reaction-based assays. Metal-ion amplification, enzyme-colorimetric reactions, and enzyme-catalyzed chemiluminescence reactions were represented by gold-ion amplification, NBT/BCIP colorimetry, and choline- and choline oxidase-based chemiluminescence reactions, respectively. The results showed that chemical reaction-based assays that were limited by conventional ICAs could be performed using the new ICA sensor combined with the water-swellable polymer. The shelf-life of the proposed sensor might depend on the stability of reagents such as stored gold ion, NBT/BCIP and luminol. According to our results, the reagent pad containing gold ion and luminol was stable until two months and three months, respectively (data not shown). If the stability of these reagents is secured for the proposed ICA strip sensor, this sensor will be widely applied to various fields.

### 3.3. CRP measurement using the new ICA sensor combined with a water-swellable polymer

We developed an advanced ICA strip sensor enabling automatic sequential reactions using the expansion effect of water-swellable polymers; gold-ion signal amplification, enzyme-colorimetric assays, and chemiluminescence reactions were successfully implemented using the developed ICA sensor combined with a water-swellable polymer. Finally, the detection of CRP in human serum was performed to evaluate the practical performance of the developed ICA sensor. CRP is a 120-kDa pentamer that represents an important inflammation biomarker and serves as an independent predictor of cardiovascular diseases (Koenig et al., 2008; Pfäfflin and Schleicher, 2009). CRP-spiked serum was used to detect CRP, and chemiluminescent signal intensity was determined 20 min after the injection of the spiked serum. As shown in Fig. 4A, target samples flowed to the test membrane after forming antigen and HRP-labeled detection-antibody complexes, and the sandwich immunoassay proceeded on the immobilized capture-antibody area. Subsequently, the chemiluminescence reagents, including luminol, choline chloride, and *p*-coumaric acid, were released from the reagent pad by expansion of the water-swellable tape. The $H_2O_2$ was generated on the immobilized choline-oxidase area located in front of the test line through the oxidation of choline chloride, and then the HRP-catalyzed chemiluminescent reaction occurred on the test line automatically. The limit of detection (LOD; blank signal +3 standard deviations) was calculated to be 0.03 ng/mL, which was superior to that of the LOD (13.65 ng/mL) observed in a conventional ICA (Fig. 4B).

In this study, the system conditions were optimized for the operation of the developed ICA sensor combined with the water-swellable polymer. Although this platform required more sample volume compared with conventional ICA, the sensitivity was improved through the automatic treatment of reagents for the signal enhancement. If conditions of the assay platform were also optimized, the sensitivity would likely be more improved. Additionally, these conditions should be modified depending on the target, the assay method and conditions. Following these optimizations, the biosensor described here will become a highly sensitive diagnostic tool.

## 4. Conclusions

In this study, we developed an advanced ICA strip sensor that

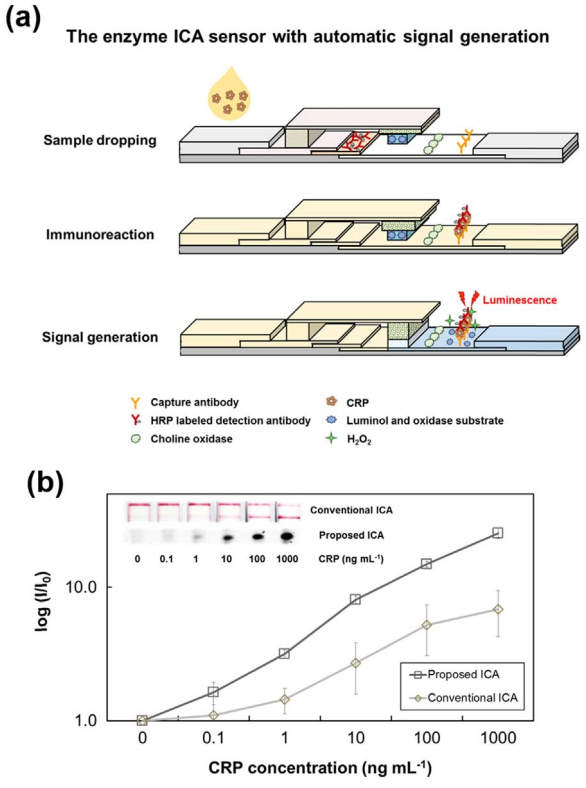


**Fig. 4.** Measurement of the CRP in human serum. (a) Schematic illustration of chemiluminescence reaction using choline oxidase. (b) Comparison of the signal intensity depending on the CRP concentration using the proposed sensor by chemiluminescence and conventional ICA sensor.

employed sequential reactions automatically. The proposed ICA strip sensor combined with a water-swellable polymer advantageously utilized the properties and characteristics of affordable water-swellable tape, thereby enabling the automatic administration of secondary reagents in a time-controlled and simple manner. The versatility of the new ICA sensor was also demonstrated using various chemical reaction-based assays, such as gold-ion amplification, NBT/BCIP-colorimetric reaction, and enzyme-catalyzed chemiluminescence. To demonstrate its practical application, the developed sensor was employed to detect CRP. The LOD for CRP measurement was found to be 0.03 ng/mL, which was relatively lower than that of conventional ICA strip sensors using AuNPs (13.65 ng/mL). Most current ICA sensors require additional support systems or complicated processes for various chemical reaction-based assays; however, this sensor, combined with a water-swellable polymer, can be easily implemented for automatic sequential reactions through a simple structural design. Also, it was confirmed that it controlled the time to switch the flow within specific periods. Moreover, all materials used for the implementation of the new ICA sensor are inexpensive and are widely used in the field of POC diagnostic sensors. Specifically, water-swellable polymers are affordable materials used in everyday life. This is a benefit over previous ICA sensors applied in sequential reactions. Based on the results of this study, we believe that the proposed sensor will be widely used in the field of POC diagnostics.

## Acknowledgments

This work was financially supported by grants from the GRL Program (NRF-2013K1A1A2A02050616), the Bio & Medical Technology Development Program (NRF-2015M3A9E2031375), and the R&D Joint Venture Program (2015K000184) of the NRF funded by the South Korean government, MSIP.

## Appendix A. Supplementary material

Supplementary data associated with this article can be found in the online version at http://dx.doi.org/10.1016/j.bios.2016.04.096.

## References

Abrams, W.R., Barber, C.A., Mccann, K., Tong, G., Chen, Z., Mauk, M.G., Wang, J., Volkov, A., Bourdelle, P., Corstjens, P.L.A.M., Zuiderwijk, M., Kardos, K., Li, S., Tanke, H.J., Niedbla, R.S., Malamud, D., Bau, H., 2007. Ann. N.Y. Acad. Sci. 1098, 375–388.
Al-Yousif, Y., Anderson, J., Chard-Bergstrom, C., Kapil, S., 2002. Clin. Diagn. Lab. Immunol. 9, 723–724.
Anfossi, L., Nardo, F.D., Giovannoli, C., Passini, C., Baggiani, C., 2013. Anal. Bioanal. Chem. 405, 9859–9867.
Blake, M.S., Johnston, K.H., Russell-Jones, G.J., Gotschlich, E.C., 1984. Anal. Biochem. 136, 175–179.
Brown, K.R., Natan, M.J., 1998. Langmuir 14, 726–728.
Chin, C.D., Laksanasopin, T., Cheung, Y.K., Steinmiller, D., Linder, V., Parsa, H., Wang, J., Moore, H., Rouse, R., Umviligihozo, G., Karita, E., Mwambarangwe, L., Braunstein, S.L., Wijert, J.v.d, Sahabo, R., Justman, J.E., E.-Sadr, W., Sia, S.K., 2011. Nat. Med. 17, 1015–1019.
Cho, J.-H., Han, S.-M., Paek, E.-H., Cho, I.-H., Paek, S.-H., 2006. Anal. Chem. 78, 793–800.
Cho, J.-H., Paek, S.-H., 2001. Biotechnol. Bioeng. 65, 725–732.
Fang, Z., Wu, W., Lu, X., Zeng, L., 2014. Biosens. Bioelectron. 56, 192–197.
Fu, E., Liang, T., Mihalic, P.S., Houghtaling, J., Ramanchandran, S., Yager, P., 2012. Anal. Chem. 84, 4574–4579.
He, M., Liu, Z., 2013. Anal. Chem 85, 11691–11694.
Hu, J., Wang, L., Li, F., Han, Y.L., Lin, M., Lu, T.J., Xu, F., 2013. Lab Chip 13, 4352–4357.
Joung, H.-A., Oh, Y.K., Kim, M.-G., 2014. Biosens. Bioelectron. 53, 330–335.
Kawde, A.-N., Mao, X., Zeng, Q., He, Y., Liu, G., 2010. Am. J. Biomed. Sci. 2, 23–32.
Kim, H.-S., Ko, H., Kang, M.-J., Pyun, J.-C., 2010. Biochip J. 4, 155–160.
Ko, Y.-J., Maeng, J.-H., Ahn, Y., Hwang, S.Y., Cho, N.G., Lee, S.-H., 2008. Electrophoresis 29, 3466–3476.
Koenig, W., Khuseyinova, N., Baumert, J., Meisinger, C., 2008. Clin. Chem. 54, 335–342.
Kost, G.J., Ehrmeyer, S.S., Chernow, B., Winkelman, J.W., Zaloga, G.P., Dellinger, R.P., Shirey, T., 1999. Chest 115, 1140–1154.
Krejcova, L., Nejdl, L., Rodrigo, M.A.M., Zurek, M., Matousek, M., Hynek, D., Zitka, O., Kopel, P., Adam, V., Kizek, R., 2014. Biosens. Bioelectron. 54, 421–427.
Leca, B.D., Verdier, A.M., Blum, L.J., 2001. Sens. Actuators B 74, 190–193.
Li, J., Zou, M., Chen, Y., Xue, Q., Zhang, F., Li, B., Wang, Y., Qi, X., Yang, Y., 2013. Anal. Chim. Acta 782, 54–58.
Liu, C.-C., Yeung, C.-Y., Chen, P.-H., Yeh, M.-K., Hou, S.-Y., 2013. Food Chem. 141, 2526–2532.
Liu, H., Crooks, R.M., 2011. J. Am. Chem. Soc. 133, 17564–17566.
Martinez, A.W., Phillips, S.T., Butte, M.J., Whitesides, G.M., 2007. Angew. Chem. Int. Ed. 46, 1318–1320.
Mirasoli, M., Buragina, A., Dolci, L.S., Simoni, P., Anfossi, L., Giraudi, G., Roda, A., 2012. Biosens. Bioelectron. 32, 283–287.
Myers, F.B., Lee, L.P., 2008. Lab Chip 8, 2015–2031.
Obubuafo, A., Balamurugan, S., Shadpour, H., Spivak, D., McCarley, R.L., Soper, S.A., 2008. Electrophoresis 29, 3436–3445.
Oh, Y.K., Joung, H.-A., Han, H.S., Suk, H.-J., Kim, M.-G., 2014. Biosens. Bioelectron. 61 (285–289), 2014.
Parolo, C., de la Escosura-Muñiz, A., MerkoÇi, A., 2013. Biosens. Bioelectron. 40, 412–416.
Pfäfflin, A., Schleicher, E., 2009. Anal. Bioanal. Chem. 393, 1473–1480.
Posthuma-Trumpie, G.A., Korf, J., van Amerongen, A., 2009. Anal. Bioanal. Chem. 393, 569–582.
Qiu, X., Thompson, J.A., Chen, Z., Liu, C., Chen, D., Ramprasad, S., Mauk, M.G., Ongagna, S., Barber, C., Abrams, W.R., Malamud, D., Corstjens, P.L.A.M., Bau, H.H., 2009. Biomed. Microdevices 11, 1175–1186.
Samsonova, J.V., Safronova, V.A., Osipov, A.P., 2015. Talanta 132, 685–689.
Song, S., Liu, N., Zhao, Z., Ediage, E.N., Wu, S., Sun, C., Saeger, S.D., Wu, A., 2014. Anal. Chem. 86, 4955–5011.
Soni, V., Mehrotra, R.N., 2003. Transit. Met. Chem. 28, 893–898.
Su, W., Gao, X., Jiang, L., Qin, J., 2015. J. Chromatogr. A 1377, 13–26.
Toley, B.J., Wang, J.A., Gupta, M., Buser, J.R., Lafleur, L.K., Lutz, B.R., Fu, E., Yager, P., 2015. Lab Chip 15, 1432–1444.
Tüdős, A.J., Besselink, G.A.J., Schasfoort, R.B.M., 2001. Lab Chip 1, 83–95.
Von Lode, P., 2005. Clin. Biochem. 38, 591–606.
Wang, S., Quan, Y., Lee, N., Kennedy, I.R., 2006. J. Agric. Food Chem. 54, 2491–2495.
Yetisen, A.K., Akram, M.S., Lowe, C.R., 2013. Lab Chip 13, 2210–2251.
Yu, C.Y., Ang, G.Y., Chua, A.L., Tan, E.H., Lee, S.Y., F.-Diaz, G., Otero, O., Rodríguez, I., Reyes, F., Acosta, A., Sarmiento, M.E., Ghosh, S., Ramamurthy, T., Yean, C.Y., Lalitha, P., Ravichandran, M., 2011. J. Microbiol. Methods 86, 277–282.
Zhang, Y., Wang, Y., Meng, J., Xie, Z., Wang, R., Kutcher, H.R., Guo, Z., 2015. J. Virol. Methods 220, 13–17.